Volume 8 Number 8 1980 Nucleic Acids Research

Precursors to 16S and 23S ribosomal RNA from a ribonuclease III⁻ strain of Escherichia coli contain intact RNase III processing sites

Peter Gegenheimer and David Apirion

Department of Microbiology and Immunology, Washington University School of Medicine, St. Louis, MO 63110, USA

Received 15 November 1979

ABSTRACT

Escherichia coli cells lacking the ribosomal RNA processing enzyme RNase III do not excise the normal RNA precursors p16a (17S) and p23a from nascent rRNA transcripts. These cells produce, instead, slightly larger p16b and p23b precursors. Digestion of p16b or p23b rRNA with RNases A plus T1 yields double-stranded fragments composed of sequences located at both the 5' and the 3' end regions of the molecules. The terminal duplex, or stem, of p16b contains sequences surrounding the site of RNase III processing which in wild-type cells produces p16a rRNA; the p23b stem likewise contains an intact RNase III cleavage site. The results confirm our earlier prediction for the structure of rRNA transcripts, and also yield a definite secondary structure for the p16 stem, which was not uniquely determined by the corresponding DNA sequence. These experiments demonstrate the absence of significant RNase III processing activity in *rnc-105* strains of *E. coli*, and implicate the participation of another endonuclease(s) in rRNA processing in mutant and wild-type cells.

INTRODUCTION

Studies on ribosomal RNA maturation in *Escherichia coli* have shown that in wild-type cells, the immediate precursors to 16S (m16) and to 23S (m23) rRNAs are p16a (17S) and p23a species generated by ribonuclease III cleavage of nascent rRNA transcripts (1,2-4). We originally proposed (4,5) that RNase III cleavage of nascent rRNA transcripts occurred in or near "stems", double-stranded regions formed by annealing of complementary sequences flanking 16S or 23S transcripts and thus separated by 1540 bases (6) or by 2904 bases (7). This hypothesis for the 16S rRNA was later confirmed by direct sequence analysis of ribosomal RNA genes (8). Since p16b and p23b of RNase III⁻ cells appeared slightly larger than their wild-type counterparts p16a and p23a (Ref. 4 and unpublished observations), we suggested that these species might arise in RNase III⁻ cells by nonspecific nucleolytic removal of single-stranded regions from larger p16 or p23-containing transcripts produced by enzymes other than

RNase III (e.g., RNases E,P, and another activity: see Refs. 9,10). In this model, p16b and p23b should contain the entire terminal duplex of p16a or p23a as well as contiguous regions derived from the portions of the primary transcript normally separated from p16a or p23a by RNase III.

To test this model, we examined the rRNA precursors p16b and p23b of RNase III$^-$ cells by RNase T1 fingerprinting and by analysis of isolated double-stranded structures. Our results indicate that p16b and p23b rRNA isolated from RNase III$^-$ cells contain additional sequences at both termini as compared to wild-type p16a and p23a and that most of these extra sequences are found in a base-paired stem which contains, and extends beyond, the site of RNase III cleavage which produces wild-type precursor p16a and p23a rRNAs. These data support our model for RNA processing in RNase III$^-$ cells, and confirm the prediction (4,5,7) that the regions of rRNA transcripts surrounding 16S and 23S RNA will anneal to form duplex recognition sites for RNase III.

MATERIALS AND METHODS

Preparation of rRNA precursors

Ribosomal RNA precursors from strain N2076 (*rnc*$^+$) or N2077 (*rnc-105*) (Ref. 11) were prepared essentially as previously described (9). At a density of about 4 x 10^8 cells/ml, cultures (10 ml) were filtered and resuspended in 10 ml tris-glucose medium containing 0.1% peptone (4). After incubation for 10 min at 30°C, chloramphenicol was added to 400µg/ml (to prevent maturation of p16 and p23 rRNA), followed 3-5 min later by neutralized $H_3^{32}PO_4$ to 1 mCi/ml. Cells were labeled for 60 min and chased for an additional 30 min by the addition of unlabeled phosphate (pH 7.0) to 20 mM. Cells were harvested, lysed, and phenol-extracted as described previously (9), with the addition of 0.2 M NaCl to the lysis buffer. RNAs were separated by gel electrophoresis, eluted (using purified RNase-free glycogen, obtained from J. Perrault, as carrier for ethanol precipitation), and purified by methylated albumin-kieselguhr (MAK) column chromatography according to Gegenheimer and Apirion (9). RNAs destined for fingerprint analysis were precipitated with purified carrier yeast RNA after the MAK column: otherwise, carrier glycogen was used.

Isolation of double-stranded stems

Double-stranded RNA was isolated by a modification (J. Perrault, personal communication) of the procedure of Perrault and Leavitt (12),

which relies on the absolute resistance of fully base-paired RNA, and the lability of non-base-paired RNA, to the action of RNases A and T1 in 0.6 M NaCl (J. Perrault, personal communication; Ref. 13). Ribosomal RNA precursors, p16b and p23b from strain N2077, containing $2x10^7$ - $2x10^8$ cts/min, and a total of 100 to 250 µg RNA, were digested in sterile 1.5 ml polypropylene microcentrifuge tubes for 15 min at 37°C with 4 U/ml RNase T1 (Calbiochem.) plus 7.5 µg/ml RNase A (Sigma) in 100 µl of 10 mM Tris-HCl/1 mM Na_2EDTA/0.6 M NaCl (pH 7.5). (The digestion conditions were chosen to give a uniform size distribution of stems. At higher enzyme concentrations the distribution was shifted to the smaller products.) Sodium dodecyl sulfate was then added to 1% (w/v), Proteinase K to 1 mg/ml, and the mixture was held at 55°C for 15 min. The digest was extracted twice with an equal volume of redistilled phenol (containing 0.1% 8-quinolinol and saturated with 10 mM Tris-HCl, pH 8.0) and the aqueous phase precipitated with 5 µg carrier RNA and 2.5 vol 95% ethanol. The resultant pellet was resuspended in gel buffer (22.5 mM Tris-borate, 0.6 mM Na_2EDTA, pH 8.3) containing 0.1 M NaCl, heated 30 sec at 50°C to disrupt RNA aggregates, and diluted with an equal volume of glycerol-EDTA-marker dye mix (9). RNAs were fractionated by electrophoresis on 1.5 mm thick polyacrylamide gel slabs (17 cm long) containing 20% acrylamide (acrylamide: bisacrylamide, 19:1), 45 mM tris-borate-EDTA gel buffer, 0.1% N,N,N',N'-tetramethylethylenediamine, and 0.05% ammonium persulfate. Gels were pre-run for 2 hr at 200V: samples were applied and run 0.5 hr at 200 V followed by 7.5 hr at 500V. Autoradiography and elution of bands have been described (9). RNAs were twice re-precipitated from 0.2 M Na-acetate, pH 5.5, washed twice with 70% ethanol, once with 95% ethanol, and finally vacuum dessicated.

Oligonucleotide analysis

Fingerprint analysis of RNAs was performed by the method of Volckaert, Min Jou and Fiers (14) as applied by Gegenheimer and Apirion (9). Electrophoresis in the first dimension was run about 75 min at 2.25 kV for rRNAs, or 50 min for smaller RNAs; homochromatography on polyethyleneimine (PEI)-cellulose plates in the second dimension was accomplished with "homomix C5" (hydrolysed 5 min) for large rRNAs or "homomix C10" (hydrolysed 10 min) for small RNAs. Working homomix solution was filtered after each use and replenished by replacing 20% of its volume with fresh homomix.

Oligonucleotides were eluted as described by Volckaert et al. (14):

eluates were dried at 43°C onto a sheet of Parafilm and washed with water. The oligonucleotides were digested in 5 µl of RNase A (0.5 mg/ml in 10 mM Tris-HCl, 1 mM Na_2EDTA, pH 7.5) in sealed capillary tubes for 6 hr at 37°C: the digests were analysed by the high resolution two-dimensional PEI thin-layer chromatography of Volckaert and Fiers (15). RNase T2 digestion of T1 oligonucleotides, or of RNase A redigestion products, was in 5 µl of 0.05 M Na-acetate (pH 4.5) containing 200 U/ml RNase T2 and 50 µg/ml RNase A, followed by two-dimensional chromatography by the method of Nishimura (16). The identity of pAp or pUp was determined by its position (16). The identity of RNase A products terminating in 2':3' cyclic GMP was determined by RNase T2 digestion and PEI chromatography as above.

Autoradiographic technique and quantitation were as described (9). The molar yield of an RNase T1 oligonucleotide in a fingerprint was determined by quantitation of the intact oligonucleotide, or of its RNase A redigestion products, after subtraction of an appropriate background. The molar yield of each oligonucleotide can be expressed as [average cts/min/nucleotide (or Gp)]/[average cts/min/nucleotide (or Gp) of a unique-sequence oligonucleotide].

Assignment of RNA sequences

The quantitative composition of each RNase T1 oligonucleotide, ascertained by RNase A redigestion, was compared with previously determined DNA sequences surrounding 16S or 23S rRNA genes on several different rRNA operons. Every RNase T1 oligonucleotide of p16b or p23b stems could be unambiguously assigned to a unique position on the DNA sequences of one or more rRNA operons (except a very few as otherwise noted in the Tables): the quantitative yield of RNase A redigestion products was in exact agreement with those predicted by the DNA sequence. The genetic nomenclature of the rrn (rRNA) operons is described in Ref. 17. The rRNAs and references for DNA sequences of the operons examined are as follows: p16 (5' side only) - rrnA, Ref. 18; p16 (5' and 3' sides) - rrn B, C. Squires and C. Squires (personal communication); rrn D, Ref. 8; rrnE, Refs. 17,18; rrnX, Ref. 8. For p23 (5' and 3' sides) - rrnD and X, Refs. 19 and 20; for p23 (5' side only) - rrnE, Ref. 17.

RESULTS

Extra Terminal Sequences of p16b and p23b rRNAs

Sequence differences between rRNA precursors of wild-type and of RNase

III⁻ cells were first examined by comparison of the RNase T1 fingerprints of each pair of RNAs. Figure 1 shows that p16b RNA is identical to p16a except for the presence of two major extra oligonucleotides, J' and J", not found in p16a [panel (a) vs (b)] and the absence of two oligonucleotides which migrate in the positions expected for the 5' and 3' ends of p16a (not shown). The compositions of these extra oligonucleotides, determined by RNase A and T2 digestion, are given in Table 1. The 5' terminus of p16b consists of equal amounts of oligonucleotides J', pUUUAUCAGp, and J", pAUUUAUCAGp, rather than pUG as in wild-type p16a rRNA. These two oligonucleotides represent the 3' terminal portion of oligonucleotide J (CUCUUUAACAAUUUAUCAGp) found in the 18S RNA species of RNase III⁻ cells (21). A new unique 3' terminus for

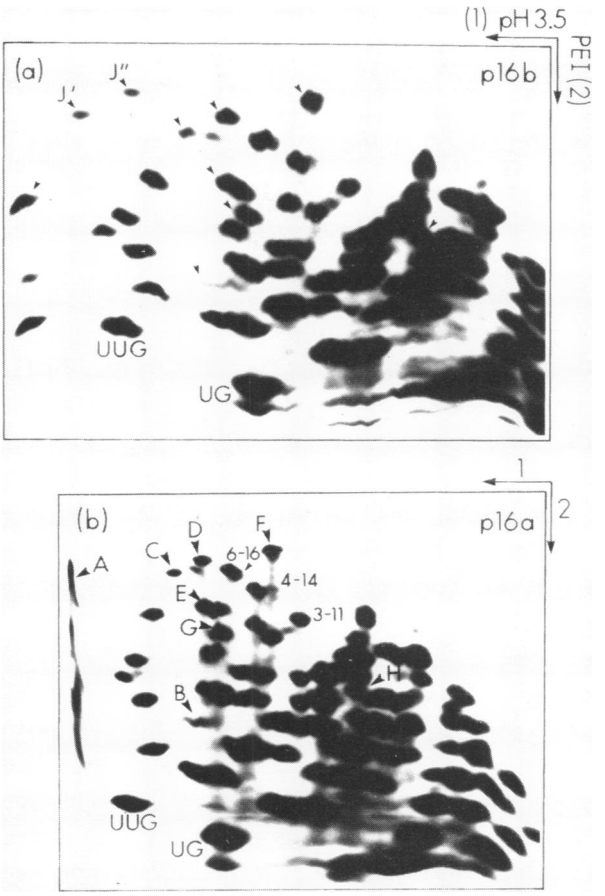

FIGURE 1. RNase T1 fingerprints of p16b and p16a rRNA. ^{32}P-labeled rRNAs (1.5-3 x 10^7 cpm) were fingerprinted as described in the Methods; an autoradiogram is shown here. Designation of oligonucleotides is according to the text; letters indicate oligonucleotides found in p16 rRNAs, and numbers, those also found in mature 16S rRNA. Unmarked arrows in panel (a) point out oligo nucleotides A through H as in panel (b): Oligonucleotides J' and J" of p16b are not detectable in p16a.

Table 1. Composition of Precursor-Specific Oligonucleotides of p16b rRNA

Oligo No.	Composition	Origin	Mole Yield
A	$(C,U_7,AAU)Gp$	p16a	0.5 - 0.7
B	$(C,U_{4-5})Gp$	p16a	0.6 - 0.9
C	$(C,U_6,AAAC,AAAU)Gp$	p16a	0.34 - 0.5
D	$(C_2,U_5,AU,AAAC,AAAU)Gp$	p16a	0.34 - 0.5
E	$(C,U_3,AC,AU,AAU)Gp$	p16a	0.46 - 0.67
F	$(C_5,U_6,AC_2,AU)AAAGp$	p16a	0.8 - 1.0
G	$(C,U_3,AU,AAC)Gp$	p16a	1.0
H	AAAAAUGp	p16a	1.0
J'	$pAU(C,U_{2-3},AU)AG$	p16b: pAUUUAUCAGp	0.34 - 0.5
J"	$pU(C,U_{2-3},AU)AG$	p16b: pUUUAUCAGp	0.34 - 0.5

The compositions of RNase T1 oligonucleotides, designated as in Fig. 1, were determined by redigestion with RNases A and T2. Oligonucleotide compositions match sequences of the rrnD operon, except oligonucleotide B from rrnE, oligonucleotide C from rrnA, and oligonucleotide H from rrnB. Sources for these sequences are listed in the Methods. The molar yield of each oligonucleotide was calculated relative to several unique oligonucleotides of m16 rRNA; the range of several determinations is given.

p16b was not located.

Similarly, Figure 2 indicates that p23b (Fig. 2(a)) contains one major T1-generated oligonucleotide, X, not found in p23a rRNA (Fig. 2(b)). Table 2 lists the compositions of several oligonucleotides of p23b (and of p23a) including some which could not be located in the catalogue of sequences reported for m23 rRNA (22). The novel oligonucleotide of p23b is present in about 0.3 mole yield, and corresponds to the sequence UCUCUCAAAUUUUCGp which can be located between 33 and 47 bases prior to the 5' side of m23 rRNA in the rrnD and X operons (19), and between 42 and 56 bases proximal to m23 in rrnE (17).

Isolation of double-stranded stems

Since only large, unique oligonucleotides can be detected by fingerprint analysis of total p16b and p23b rRNAs after digestion with RNase T1, this analysis could yield only very general data about the extent of extra sequences not present in the corresponding wild-type molecules. To obtain detailed information on the extent of such extra sequences, we attempted to isolate them directly. We previously proposed that in nascent rRNA transcripts the precursor-specific regions flanking

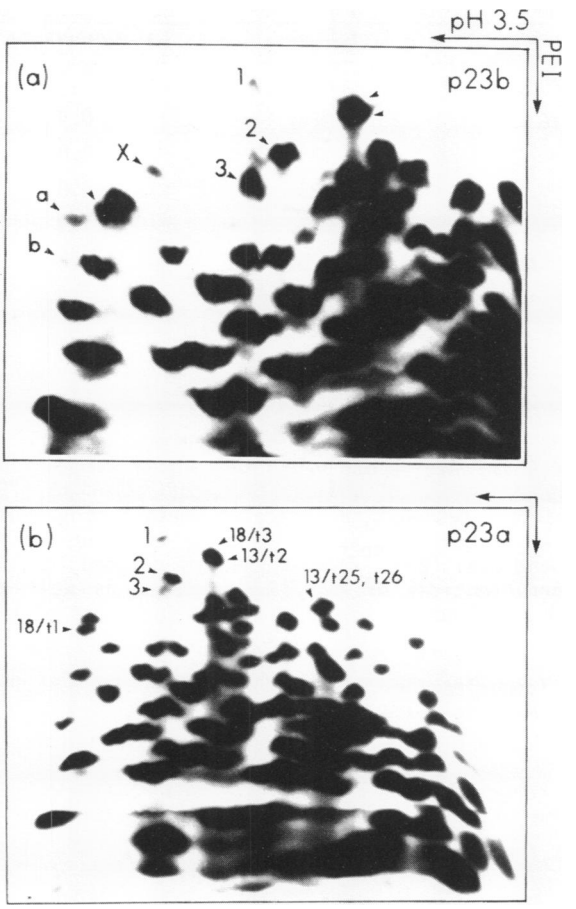

FIGURE 2. RNase T1 fingerprints of p23b and p23a rRNAs. ^{32}P-labeled rRNAs (1.5-3 x 10^7 cpm) were fingerprinted according to the Methods. Oligonucleotides X, a, and b of p23b rRNA are not detectable in p23a rRNA. Oligonucleotides 1, 2 and 3 are common to both molecules (oligonucleotide 3 of p23a is typically more prominent than in this fingerprint (panel (b)). All the other oligonucleotides are also found in mature 23S rRNA.

p16 and p23 rRNA are hydrogen-bonded in duplex stems from which mature rRNAs loop out (4,5). Accordingly, we attempted to isolate such stems by digestion of p16b or p23b rRNA with RNases T1 and A in buffer containing 0.6 M NaCl. The purified products were fractionated by electrophoresis on a 20% polyacrylamide gel, an autoradiogram of which is shown in Figure 3, where it can be seen that each RNA gives rise to several RNase-resistant products. Those products subsequently shown to contain precursor-specific sequences are numbered in order of decreasing size. Other products — the smallest band in each lane — were also examined but were found not to contain any precursor-specific sequences.

Each p16b product was fingerprinted; fingerprints of bands I through

Table 2. Composition of Oligonucleotides of p23b rRNA

Oligo No.	Composition	Origin	Mole Yield
18/t3	$(C_3,U_4,AC_2,AAU,AAAU)G$	m23	0.9
13/t2	$(C,U_3,AC_3,AU_2,AAC)G$	m23	0.9
13/t25	$(C_3,U_2,AC_2,AAC)G$	m23	0.8
13/t26	$(C_5,U,AC,AU)AAG$	m23	0.8
18/t1	$(C_2,U_{3-4},AU,AAU)G$	m23	1.3
2	$(C_{1-2},U_6,AC,AU_{1-2},AAAAAC)AG$	(p23a,b)	0.6
3[a]	$C_2,U_7,AC,AU_{1-2},AAU,"A_4U"^b,G,AG$	(p23a,b)	0.3
a	$(C_2,U_3,AU_2)G$	(p23b)	0.15
X	$(C_{4-5},U_6,AAAU)G$	p23b: UCUCUCAAAUUUUCG	0.2 - 0.4

Oligonucleotides from p23b rRNA fingerprints, numbered as in Fig. 2, were further digested with RNase A. Oligonucleotides whose composition corresponded with previously sequenced oligonucleotides of m23 rRNA (22) are so indicated: their numerical designation indicates whether they arose from the 18S or the 13S fragment of 23S, as well as the oligonucleotide number assigned by Branlant and Ebel (22). The sequence of oligonucleotide X is from rrnD: other oligonucleotides of p23 (2,3, and a; as well as oligonucleotide 1 in Fig. 2) could not be assigned to DNA sequences of the rrnD, E, or X operons.

[a] contains two different oligonucleotides.
[b] "A_4U" probably contains a modified base.

IV are shown in Figure 4. The sequence of each oligonucleotide (inferred from its composition) and its molar yield are given in Table 3. All the oligonucleotides of bands I to IVb are compatible with known DNA sequences. From the structure presented in Figure 5, it can be seen that the five bands in fact comprise a nested set of stems, all of which start in the same position ("I-IV" at the bottom of Figure 5), but that each successive species contains extra sequences located closer to mature 16S RNA. Stem I is 39 base pairs in length; stems II, III, and IV can be derived from stem I by cleavage at mismatched or unpaired bases in the duplex stalk. Stem IVb is almost identical to stem IV: its fingerprint (not shown) also contains three oligonucleotides (numbers 3,7, and 19 in Table 3) which are probably not part of the stem per se. The principal site at which RNase III cleaves 30S rRNA transcripts to give p16a rRNA has been determined (see 2,23). All five stems contain 13 extra bases preceding the 5' terminus of p16a rRNA, and 11 extra bases following its 3' terminus.

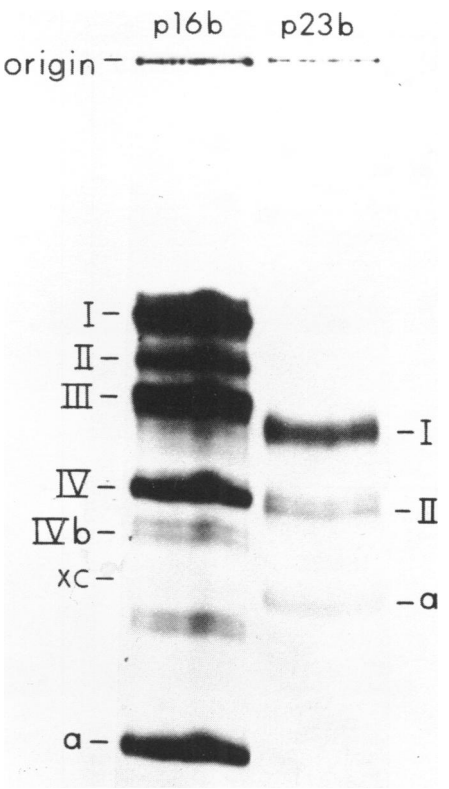

FIGURE 3. Isolation of double-stranded stems. ^{32}P-labeled p16b rRNA (90µg, 7.6×10^7 cts/min) or p23b rRNA (250µg, 2.3×10^7 cts/min) were digested with RNases A plus T1 as described in the Methods. The RNase-resistant material was separated by electrophoresis on a 20% polyacrylamide gel, an autoradiogram of which is shown here. Roman numerals denote RNA species whose sequences were found to correspond to the termini of p16b or p23b, respectively. Band a in each lane was found not to contain these sequences. XC marks the position of the xylene cyanol FF marker dye.

The extent of each stem of p16b was determined by aligning its constituent oligonucleotides, listed in Table 3, according to known DNA sequences (see Methods). We locate the base of stems I through IVb at positions -127 and 44' in Figure 5, because all stems contain AUCAGp rather than the 5' end of p16b, p(A)UUUAUCAGp (positions -131 to -123), and have AUp instead of the AUGp at positions 43' to 45'. The top of stem I is placed at nucleotides -88 and 5' since this species includes AUUCUUp instead of AUUCUUAACGp, positions -93 to -84, and has AAAGp rather than ---CCUUAAAGp at positions 1' to 8'. Similar reasoning yielded the assignments of cleavages which generate stems II, III, and IV. The termini of stem IVb differ from those of stem IV only in the substitution of CACp for CACUp (-108 to -105), as indicated in Figure 5.

Double-stranded stems of p23b rRNA were analysed similarly to those of p16b. Fingerprints of stems I and II are shown in Figure 6, and

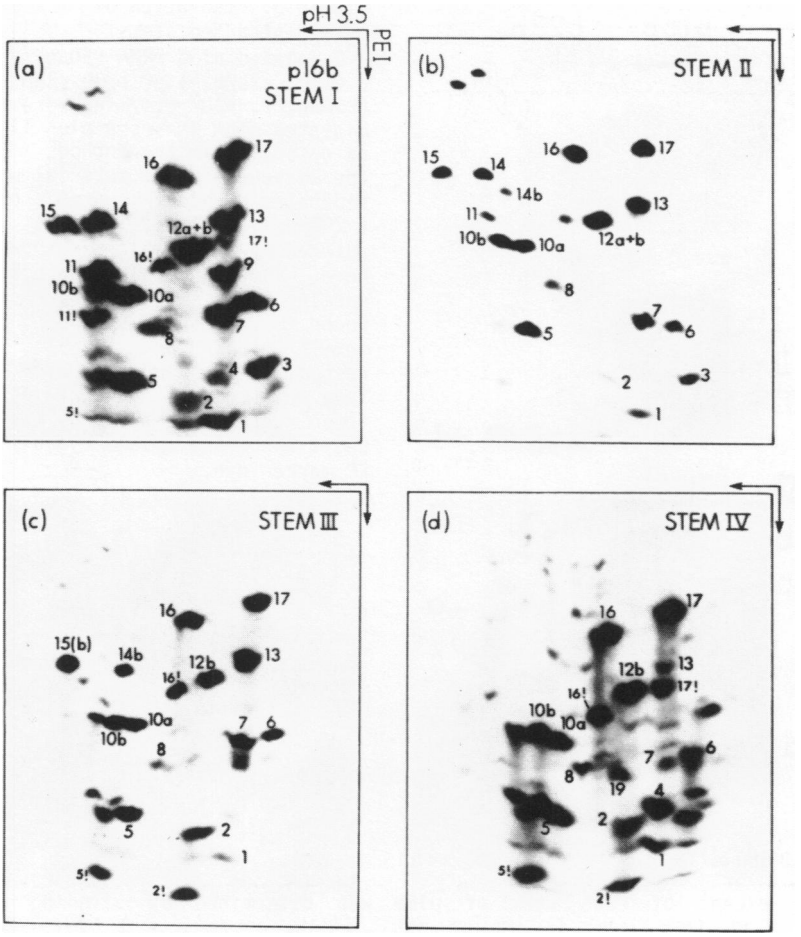

FIGURE 4. RNase T1 fingerprints of duplex stems from p16b rRNA. Stems I through IV correspond to bands I through IV in Fig. 3. An exclamation point indicates that the oligonucleotide terminates with cyclic Gp (e.g. 16! represents 16 with cyclic Gp). Oligonucleotides not numbered were also analysed but were present in low amounts and did not contain sequences from the terminal regions of p16b rRNA. The spots near oligonucleotides 5 and 10b, in panels (c) and (d), have compositions similar to 5 and 10b. Oligonucleotide 2 is present in all fingerprints but did not reproduce well in (b).

compositional analysis is given in Table 4. The structure of these stems is shown in Figure 7; again, it is apparent that stem II is a subset of I. Stem I is 27 base pairs long, and includes 8 bases of the 5' end and 10 bases of the 3' end of mature m23 rRNA. The site at which RNase III

Table 3. Sequences and Molar Yields of Oligonucleotides from p16b Stems

Oligo No.	Deduced Sequence	Stem I	Stem II	Stem III	Stem IV	Stem IVb
1	G	2.9 (3)	1.9 (2)	1.4 (2)	1.6 (2)	2.4 (2)
2	AU	1.3 (1)	1.2 (1)	1.8 (1.5)	1.2 (1)	0.5 (0)
3	CG	1.5 (1)	1.2 (1)	--[a] (0)	0.3 (0)	1.0 (0)[b]
4	AG	0.4 (0)	0.2 (0)	0.2 (0)	0.9 (1)	0.5 (1)
5	UG	2.6 (3)	3.1 (3)	2.8 (3)	2.8 (3)	3.0 (3)
7	AAG	2.1 (2)	1.4 (1)	1.3 (1)	0.1 (0)	0.8 (0)
6	CAG (rrnD,E,X)	1.0 (1)	0.7 (1)	0.5 (1)	0.3 (0)	0.2 (0)
8	UAG (rrnB) [c]	0.2	0.6	0.3	0.2	0.4
9	AAAG	0.7 (1)	-- (0)	-- (0)	-- (0)	-- (0)
10a	UCUG	0.9 (1)	1.0 (1)	0.8 (1)	0.8 (1)	0.6 (1)
10b	AUUG	1.1 (1)	1.2 (1)	1.0 (1)	1.1 (1)	0.9 (1)
11	AUUCUU	1.2 (1)	0.2 (0)	-- (0)	-- (0)	-- (0)
12a	AUACG	1.2 (1)	0.7 (1)	-- (0)	-- (0)	-- (0)
12b	AUCAG	1.1 (1)	0.7 (1)	1.1 (1)	1.0 (1)	0.8 (1)
13	CACUCG	1.1 (1)	1.0 (1)	1.2 (1)	-- (0)	0.2 (0)
14	UACUUUG (rrnB,D,X)	0.8 (1)	0.4 (1)	-- (0)	-- (0)	-- (0)
15	UUCUUUG (rrnE) [c]	0.3	0.4	0.6[d]	--	--
14b	ACUUUG (rrnB,D,X)	-- (0)	0.2 (0)	0.3 (1)	-- (0)	-- (0)
15b	UCUUUG (rrnE) [c]	--	--	-[d]	--	--
16	ACAAUCUG	1 (1)	1 (1)	1 (1)	1 (1)	1 (1)
17	CUCACACAG	1 (1)	1 (1)	1 (1)	1 (1)	1 (1)
18	CACU	-- (0)	-- (0)	-- (0)	0.5 (1)	0.2 (0)
19	(U,C)G	-- (0)	-- (0)	-- (0)	0.2 (0)	1.1 (0)[b]
20a+b	CAC	-- (0)	-- (0)	-- (0)	-- (0)	0.6 (1)
Distribution[e]:		0.28	0.11	0.32	0.23	0.06

For each oligonucleotide from RNase T1 fingerprints of p16b stems I through IVb, numbered as in Fig. 4, oligonucleotide composition and sequence assignment were performed according to the Methods. In each sequence, RNase A redigestion products greater than one base long are underlined. The molar yield of each oligonucleotide is expressed relative to oligonucleotides 16 and 17, and is followed in parentheses by the yield expected from the structure of Fig. 5.

[a] less than 0.1 mole
[b] probably derived from Stem III
[c] oligonucleotides occupying the same position but differing by a single base change in the two groups of rRNA operons indicated. UACUUUG is p16 precursor-specific oligonucleotide B', and UUCUUUG is B (see Text)
[d] the value assigned to 15 (UUCUUUG) probably represents 15b (UCUUUG)
[e] amount of each stem as a fraction of the total (adjusted for differences in size), calculated from the average cts/min of Gp from unitary oligonucleotides of each stem

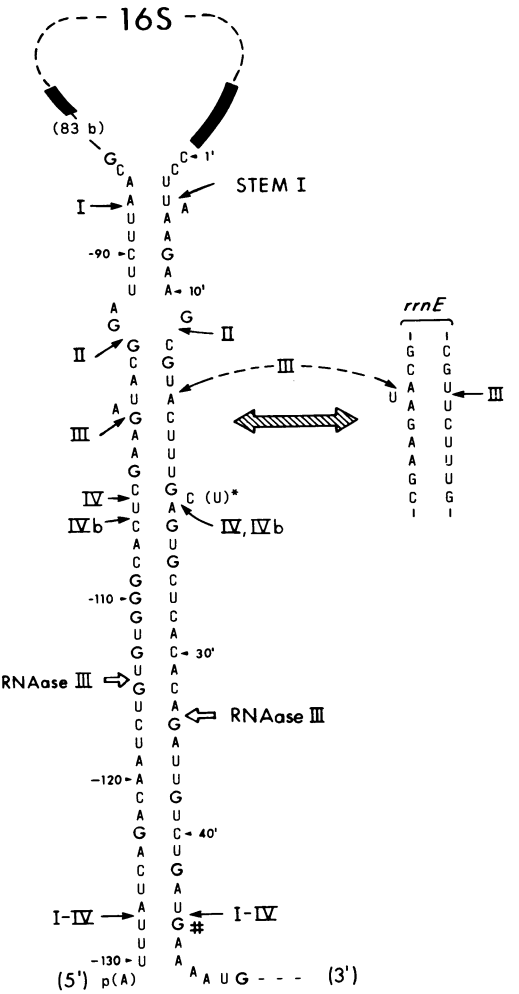

FIGURE 5. Sequence and secondary structure of stems isolated from p16b rRNA. RNase-resistant oligonucleotides (from Table 3) are arranged according to the DNA sequences of the rrnD and X operons (8); the homologous sequence in rrnE (right) is from Ref. 18. Arrows indicate the extent of the isolated stems I through IVb (Figure 3): they are placed as described in the text. To facilitate reference to the text and to Table 3, the terminal G of each T1 oligonucleotide is in bold face, and nucleotide positions prior to the 5' end of m16 (negative numbers) and past the 3' end (primed numbers) are numbered. The solid bars indicate the termini of mature 16S rRNA. Location of the RNase III cleavage site in 30S rRNA, between positions -114 and -115 and 33'/34', is from Refs. 2 and 23.
*, C is replaced by U in rrnB (C. Squires and C. Squires, personal communication);# , the sequence of rrnB and E begins to diverge from that shown here.

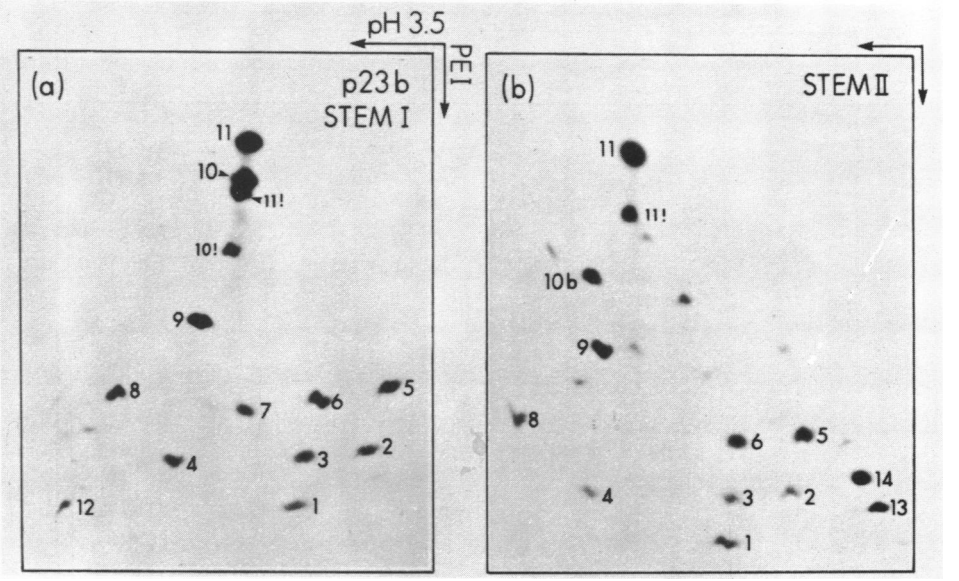

FIGURE 6. RNase T1 fingerprints of duplex stems from p23b rRNA. Stem I is band I of Figure 3, and Stem II is band II. Details as in Figure 4.

cleavage produces p23a rRNA (20) is contained within this stem, which extends 10 bases past the 3' side, and 12 bases before the 5' side of the RNase III cleavage site (see Figure 7).

The base of stem I can be located at positions -19 and 18' since this species contains AAACAUCUUCG (-19 to -9) and, although lacking UUUUG(16' to 20'), has close to 3 moles of Up, which probably correspond to UUUp (16' to 18': see Table 4 and Fig. 7). The Gp at -20 was excluded since stem I contains only 4-4.5 G's, rather than 5-5.5 (Table 4). The top of stems I and II are placed at +8 and -10', within mature m23 rRNA, in accord with the oligonucleotide content and Gp yield of the stems. Since we estimate that half the sequences at 13' to 15' are CUG, and half GUG, cleavage between positions 13' and 14' would result in the loss of 0.5 mole CUG and 0.5 mole UG, as observed in Table 4.

DISCUSSION

The immediate precursors to 16S and to 23S rRNAs, when isolated from an RNase III- strain of *E. coli*, contain extra sequences not found in

Table 4. Sequences and Molar Yields of Oligonucleotides from p23b Stems

Oligo No.	Deduced Sequence	Stem I	Stem II
1	G	3.8 (4.5)	4.7 (4.5)
2	CG	1.3 (0)	1.4 (0)
3	AG	1.0 (1)	1.4 (1)
4	UG	1.5 (1.5)	1.2 (1)
5	CCG	1.0 (1)	2.1 (1)
6	AAG	0.9 (1)	1.0 (1)
7	(CUG)[a]	0.6 (0.5)	--[b] (0)
8	UUG	1.0 (1)	1.4 (1)
9	UUAAG	1.1 (1)	0.8 (1)
10	AAACAUCUUCG	1 (1)	-- (0)
10b	AUCUUCG	-- (0)	0.8 (1)
11	CUUAACCUUACAACG	1.0 (1)	1.1 (1)
12a+b	U[c]	2.3 (3)	-- (0)
13	AC	--	1.6 (0)
14	AAC	--	2.1 (0)
--	C	n.d.[d] (1)	n.d. (2)
Distribution[e]:		0.74	0.26

The sequence and yield of each oligonucleotide of p23b stems I and II, designated according to the fingerprints in Fig. 6, were determined as described in the Methods. RNase A redigestion products of length greater than one are underlined. Molar yields were determined relative to the yield of oligonucleotide 10; the value in parentheses is the yield expected from Fig. 7. Because GUG and CUG are proposed to occur at the same position in approximately equal amounts (see Fig. 7), the calculated yields include 0.5 mole each of G, UG, and CUG.

[a] Proposed (see text and Fig. 7)
[b] less than 0.1 mole
[c] 12a and 12b contain different amounts of Up; may represent UUUp and UUp
[d] not detected
[e] amount of each stem as a fraction of the total (as in Table 3)

the corresponding wild-type precursors. Most of these sequences are located within a terminal duplex region formed by the annealing of complementary sequences located at either end of the precursor molecule and separated by 1540 or by 2904 nucleotides. The double-stranded stem of p16b rRNA contains the intact sequence within which RNase III cleaves nascent rRNA transcripts to produce p16a rRNA; the p23b stem similarly contains an intact RNase III processing site.

Sequence heterogeneity of rRNA transcripts

The p16b rRNA population includes transcripts representative of at

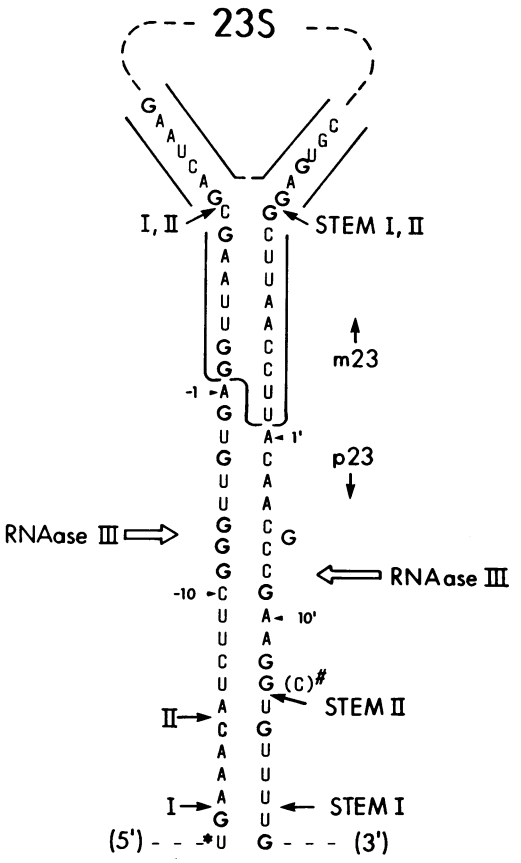

FIGURE 7. Sequence and secondary structure of stems isolated from p23b rRNA. RNase-resistant oligonucleotides from Table 4 are aligned according to the sequence of rrnD and X (19,20). The terminal sequences of mature 23S (m23) rRNA (Refs. 22,24) are enclosed within solid lines. The site of RNase III cleavage is between positions -7/-8 and 8'/9' (20). Other details are as in the legend to Figure 5. Oligonucleotide X of p23b (see text and Table 2) is located 12 bases to the left of the sequences shown here, at positions -33 to -47 (rrnD,X) or -42 to -56 (rrnE), and hence is not shown in this figure.
*, preceding sequence in rrnE is divergent through this position. # , position of proposed sequence heterogeneity (see text and Table 4); A is found here in rrnX but was not detected in our stems I or II.

least four ribosomal RNA operons for which sequence information is available. In the isolated p16b stems we detect both oligonucleotide B and its homologue B' (see Table 3). Oligonucleotide B corresponds to the rrnE operon: oligonucleotide B' can be transcribed from the rrnB, D, and X operons. We also detected in p16a and p16b the homologous oligonucleotides C, transcribed from rrnA, and D, from rrnB, D, E, and X. Oligonucleotides A,E, and F, furthermore, are present in yields suggestive of their presence in only 3 to 5 of the 7 rRNA operons.

Similar heterogeneity exists in p23b transcripts. Oligonucleotide X could be present in up to four transcription units, including rrnD, E, and X (17,19). The other p23b oligonucleotides (not found in m23) listed in Table 4 are also present in much less than a molar yield, suggesting that

there might be considerable sequence heterogeneity in the precursor portions of p23b genes. It is noteworthy, however, that the sequences involved in base-pairing are largely conserved (see Fig. 7).

Secondary structure of stems

Since RNases A and T1 attack only nucleotide residues which are not base-paired in 0.6 M NaCl, the secondary structure of p16b and p23b stems can be deduced from the locations at which they are cleaved. As drawn in Fig. 5, the secondary structure of the p16b stem is such that all the cleavages we detect occur at sites where a single unpaired base "bulges" out (top of stems I, III, IV) or at a mismatch (top of stem II: bottom of all stems). This secondary structure is similar to that proposed by Young and Steitz (8), except for the region between the end of stems I and II at the 5' side of 16S. The structures proposed by Dahlberg et al. (25) and by Sekiya and Nishimura (26) differ considerably from the present findings, in that those models depict as single-stranded large stretches of sequences we find to be nuclease-resistant. Analysis of the p16b stem has thus allowed assignment of a particular secondary structure to a sequence for which numerous configurations were possible. While we cannot exclude the possibility that some p16 terminal regions might exist in nuclease-labile configurations, we have established that those termini which are nuclease-resistant do exist predominantly as the structure shown in Fig 6.

The longest nuclease-resistant region of p23b is stem I. Most p23b molecules probably do not have longer stems, because p23b-specific oligonucleotide X, located 14 bases before stem I, is found in much less than a molar yield in intact p23b rRNA.

None of the nuclease-resistant material from p23 or p16, longer than 20 base pairs, contained sequences derived from the mature rRNA regions. Apparently, then, m16 and m23 rRNAs of E. coli, although possessing considerable secondary structure, do not contain lengthy duplexes which are stable under the conditions employed here. It is interesting that the terminal duplex of p23 does, however, continue into m23 sequences for 8 contiguous base pairs. [While these experiments were in progress, Robertson and Barany (27) presented evidence that some of the double-stranded RNA molecules isolated from total cellular RNA of an RNase III$^-$ RNase P$^-$ mutant strain correspond to rDNA sequences, flanking 16S rRNA, which could produce stems.]

Absence of RNase III processing activity

All of the ^{32}P-labeled rRNA species in the experiments described

here were present in the form of p16 and p23 molecules, because cells were labeled after treatment with chloramphenicol, which blocks conversion of p16 and p23 precursors into the mature m16 and m23 species (1,4). If the RNase III$^-$ strain studied here contained any functional residual RNase III activity, we would expect to find that some of the p16 and p23 molecules were p16a and p23a species which were produced by RNase III cleavages, and which would give rise to short stems containing some characteristic unique terminal T1 oligonucleotides. However, all the nuclease-resistant, double-stranded stems isolated from p16 and p23 rRNA of an RNase III$^-$ strain of E. coli contain the intact sequences at which RNase III cleaves nascent rRNA transcripts, and none contains T1 oligonucleotides which would have resulted from RNase III cleavage. The double-stranded RNAs seen in Fig. 3 range from about 10 to about 40 base pairs in length. In this range no major band was terminated by an RNase III cleavage; in particular, the largest stem from wild-type p16a rRNA, which would contain 23 base pairs, was not found, nor were its terminal oligonucleotides detected in any p16 material that was analyzed. Of the minor bands which we did not analyse, all are present in amounts much less than p16b stem IVb (see Fig. 3), which represents only 6% of the total p16 stems (Table 3), hence the amount of RNase III-cleaved p16a sequences in rnc-105 strains can be no greater than about 5% of the total. A similar upper limit can be set for the presence of p23a sequences in the p23b material. Since cultures were labeled for 60 min (equivalent to 1 generation) and chased for 30 min, substantial nucleolytic processing, if any, of the precursor rRNAs could have been completed. [The chloramphenicol treatment itself does not inhibit RNase III activity (4).] We conclude from this evidence that rnc-105 cells contain insignificant amounts of RNase III rRNA processing activity, and that the p16b and p23b precursor rRNAs are formed from larger rRNA transcripts in such cells by the action of other nucleases.

Conclusion

The data provide direct evidence that complementary sequences which surround 16S or 23S sequences in E. coli ribosomal RNA transcripts, can anneal, at least in vitro, to form double-stranded stems. The secondary structure of the stems can be ascertained from their susceptibility to nuclease digestion. These stems contain processing sites for RNase III, the enzyme which in wild-type cells introduces the first endonucleolytic

cuts into nascent rRNA transcripts. In cells lacking RNase III, p16b and p23b ribosomal RNA precursors are formed which contain additional stem sequences extending beyond the RNase III cleavage sites. These precursors are probably generated by non-specific nucleolytic trimming of larger species which were cleaved from nascent transcripts by other rRNA processing endonucleases (4, 10). Like wild-type p16a and p23a precursors, however, p16b and p23b rRNAs are converted in vivo to functional m16 and m23 rRNAs (see Refs. 4 and 28). Prior cleavage by RNase III is hence not required for the maturation process which converts these slightly larger than normal p16b or p23b precursors into mature 16S and 23S rRNAs. The viability of RNase III$^-$ strains thus results from their capacity to produce p16b and p23b precursor rRNAs which resemble wild-type p16a and p23a sufficiently to be recognized and processed to mature m16 and m23 ribosomal RNAs.

ACKNOWLEDGMENTS

We benefited from numerous discussions of stems with Dr. Jacques Perrault, who also provided experimental protocols and gave a critical reading to this manuscript. Drs. M. Nomura, C. Squires and C. Squires, and R.A. Young and J.A. Steitz very generously communicated DNA sequence information, and Dr. Steitz the p23 RNase III cleavage data, prior to publication. This study was supported by NIH grants GM 25890 and GM 19821, and NSF grant PCM 76-81665.

REFERENCES

1. Pace, N.R. (1973) Bacteriol. Rev. 37, 562-603
2. Ginsburg, D. and Steitz, J.A. (1975) J. Biol. Chem. 250, 5647-5654
3. Gegenheimer, P. and Apirion, D. (1975) J. Biol. Chem. 250, 2407-2409
4. Gegenheimer, P., Watson, N. and Apirion, D. (1977) J. Biol. Chem. 252, 3064-3073
5. Gegenheimer, P., Watson, N. and Apirion, D. (1976) in Molecular Mechanisms in the Control of Gene Expression, Nierlich, D.P., Rutter, W.J. and Fox, C.F., Eds., pp. 405-410, Academic Press, New York
6. Brosius, J., Palmer, M.L., Kennedy, P.J. and Noller, H. (1978) Proc. Natl. Acad. Sci. USA 75, 4801-4805
7. Brosius, J., Dull, T.J., and Noller, H.F. (1980) Proc. Natl. Acad. Sci. USA 77, 201-2048.
8. Young, R.A. and Steitz, J.A. (1978) Proc. Natl. Acad. Sci. USA 75, 3593-3597
9. Gegenheimer, P. and Apirion, D. (1978) Cell 15, 527-539
10. Apirion, D., Ghora, B.K., Plautz, G., Misra, T. and Gegenheimer, P. (1980) in Transfer RNA. Part 2: Biological Aspects, Soll, D., Abelson, J. and Schimmel, P., Eds., Cold Spring Harbor Laboratory, New York, pp. 139-154.

11. Apirion, D. and Watson, N. (1975) J. Bacteriol. 124, 317-324
12. Perrault, J. and Leavitt, R.W. (1977) J. Gen. Virol. 38, 35-50
13. Mittelstaedt, R., Oppermann, H. and Koch, G. (1975) Arch. Virol. 47, 381-392
14. Volckaert, G., Min Jou, W. and Fiers, W. (1976) Anal. Biochem. 72, 433-446
15. Volckaert, G. and Fiers, W. (1977) Anal. Biochem. 83, 228-239
16. Nishimura, S. (1972) Prog. Nucl. Acids Res. Mol. Biol. 12, 49-85
17. Morgan, E.A., Ikemura, T., Post, L.E. and Nomura, M. (1980) in Transfer RNA. Part 2: Biological Aspects, Soll, D., Abelson, J. and Schimmel, P., Eds., Cold Spring Harbor Laboratory, New York, in press
18. de Boer, H.A., Gilbert, S.F. and Nomura, M. (1979) Cell 17, 201-209
19. Young, R.A., Macklis, R. and Steitz, J.A. (1979) J. Biol. Chem. 254, 3264-3271
20. Bram, R.J., Young, R.A. and Steitz, J.A. (1980) Cell 19, 393-401.
21. Gegenheimer, P. and Apirion, D., manuscript in preparation
22. Branlant, C. and Ebel, J.-P. (1976) J. Mol. Biol. 111, 215-256
23. Lund, E. and Dahlberg, J.E., (1979) Proc. Natl. Acad. Sci. USA 76, 5480-5484
24. Takanami, M. (1967) J. Mol. Biol. 23, 135-148
25. Dahlberg, A.E., Dahlberg, J.E., Lund, E., Tokimatsu, H., Rabson, A.B., Calvert, P.C., Reynolds, F., and Zahalak, M. (1978) Proc. Natl. Acad. Sci. USA 75, 3598-3602
26. Sekiya, T. and Nishimura, S. (1979) Nucl. Acids Res. 6, 575-592
27. Robertson, H.D. and Barany, F. (1979) in Proceedings of the 12th FEBS Congress, Pergamon Press, Oxford, pp. 285-295
28. Sprague, K.U. and Steitz, J.A. (1975) Nucl. Acids Res. 2, 787-798